

**Supplementary Information for “Influences of large-scale convection and moisture source on monthly precipitation isotope ratios observed in Thailand, Southeast Asia”**

Zhongwang Wei<sup>1</sup>, Xuhui Lee<sup>1,2</sup>, Zhongfang Liu<sup>3</sup>, Uma Seeboonruang<sup>4</sup>, Masahiro Koike<sup>5</sup>, Kei Yoshimura<sup>5,6</sup>

<sup>1</sup>School of Forestry and Environmental Studies, Yale University, New Haven, Connecticut, USA.

<sup>2</sup>Yale-NUIST Center on Atmospheric Environment, Nanjing University of Information Science & Technology, Nanjing, Jiangsu, China.

<sup>3</sup>State Key Laboratory of Marine Geology, Tongji University, Shanghai 200092, China

<sup>4</sup>Faculty of Engineering, King Mongkut's Institute of Technology Ladkrabang, Thailand

<sup>5</sup>Institute of Industrial Science, The University of Tokyo, Komaba, Tokyo, Japan.

<sup>6</sup>Atmosphere and ocean research institute, The University of Tokyo, Kashiwa, Chiba, Japan.

Corresponding author: Zhongwang Wei, School of Forestry and Environmental Studies, Yale University, New Haven, Connecticut, USA. (zhongwang.wei@yale.edu)

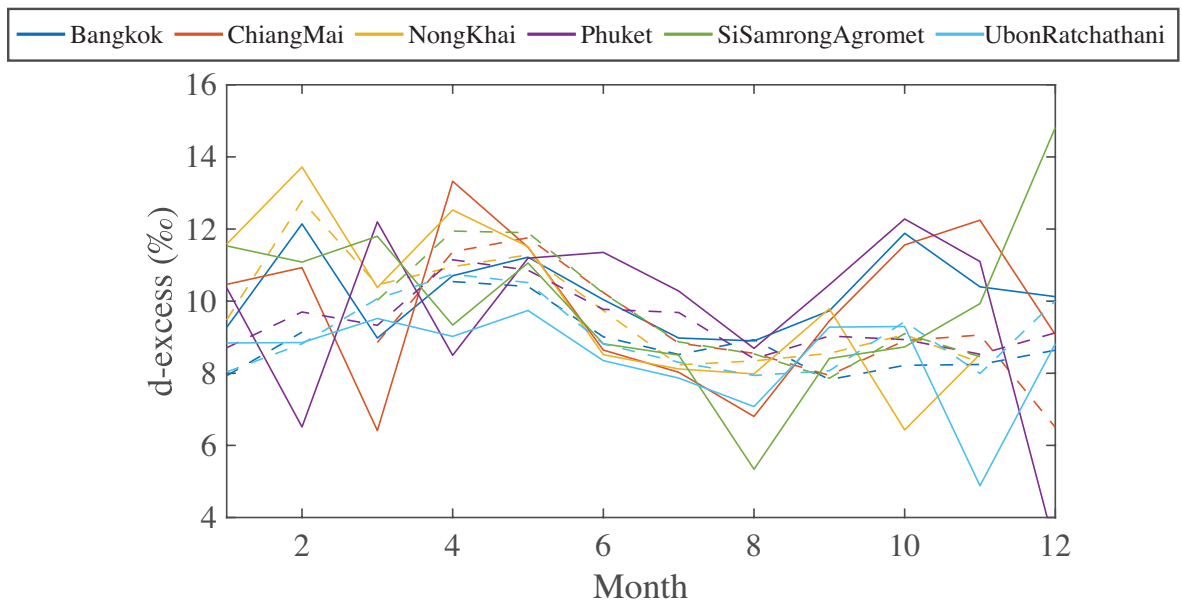


Figure S1. Multi-year mean seasonal variations of site-measured (solid lines) and IsoGSM simulated (dash lines) precipitation d-excess.

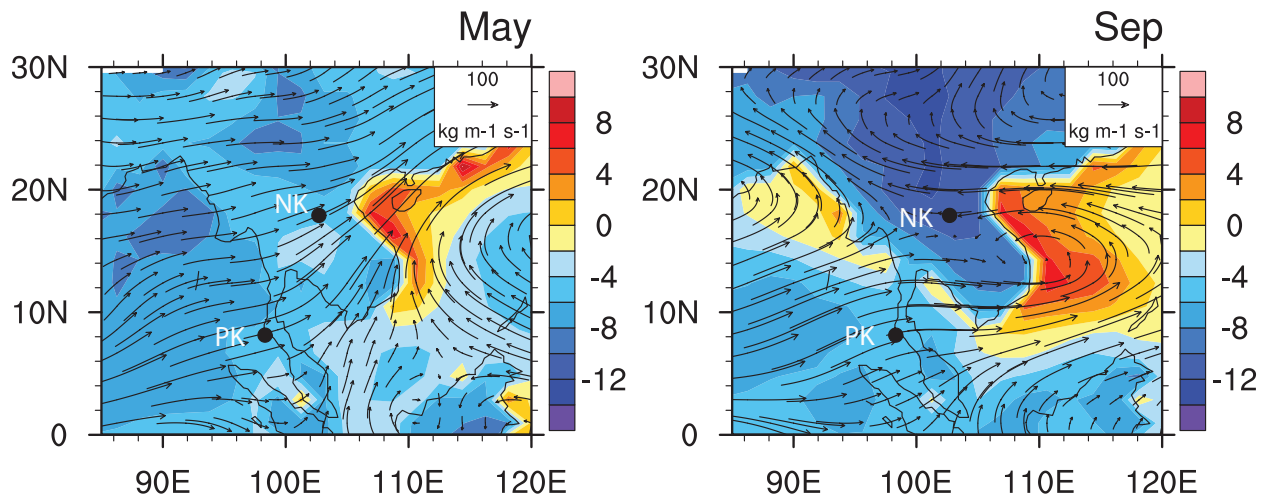


Figure S2. IsoGSM-simulated spatial distribution of mean vertical integral water vapor (water vapor transport integrated between the surface layer to 300 hPa level) transport (plotted as vectors) and mean evaporation  $\delta^{18}\text{O}$  isotope ratios (plotted as shading), for May and September.

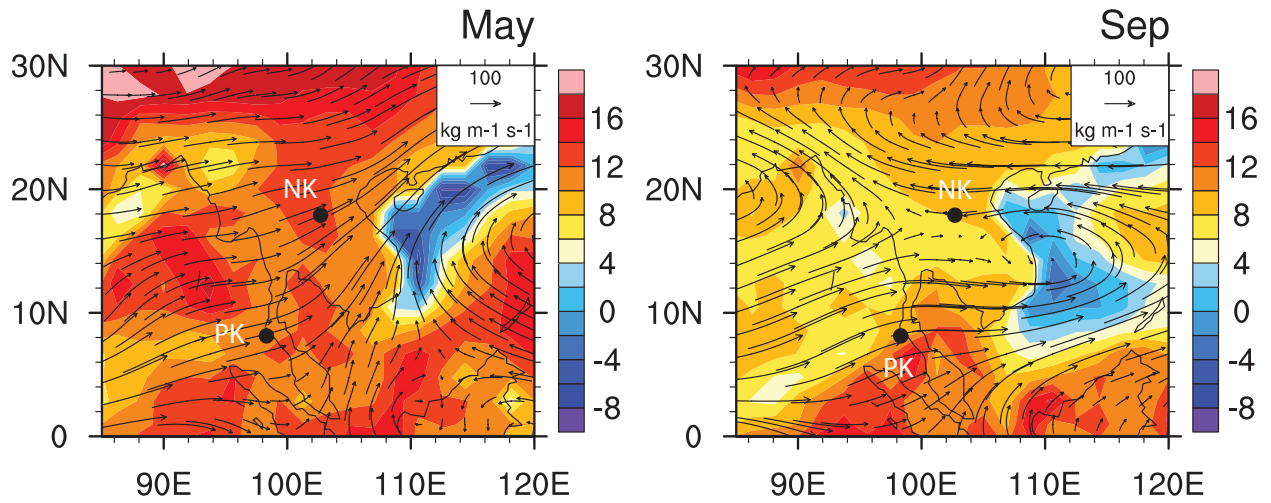


Figure S3. IsoGSM-simulated spatial distribution of mean vertical integral water vapor (water vapor transport integrated between the surface layer to 300 hPa level) transport (plotted as vectors) and mean evaporation d-excess isotope ratios (plotted as shading), for May and September.

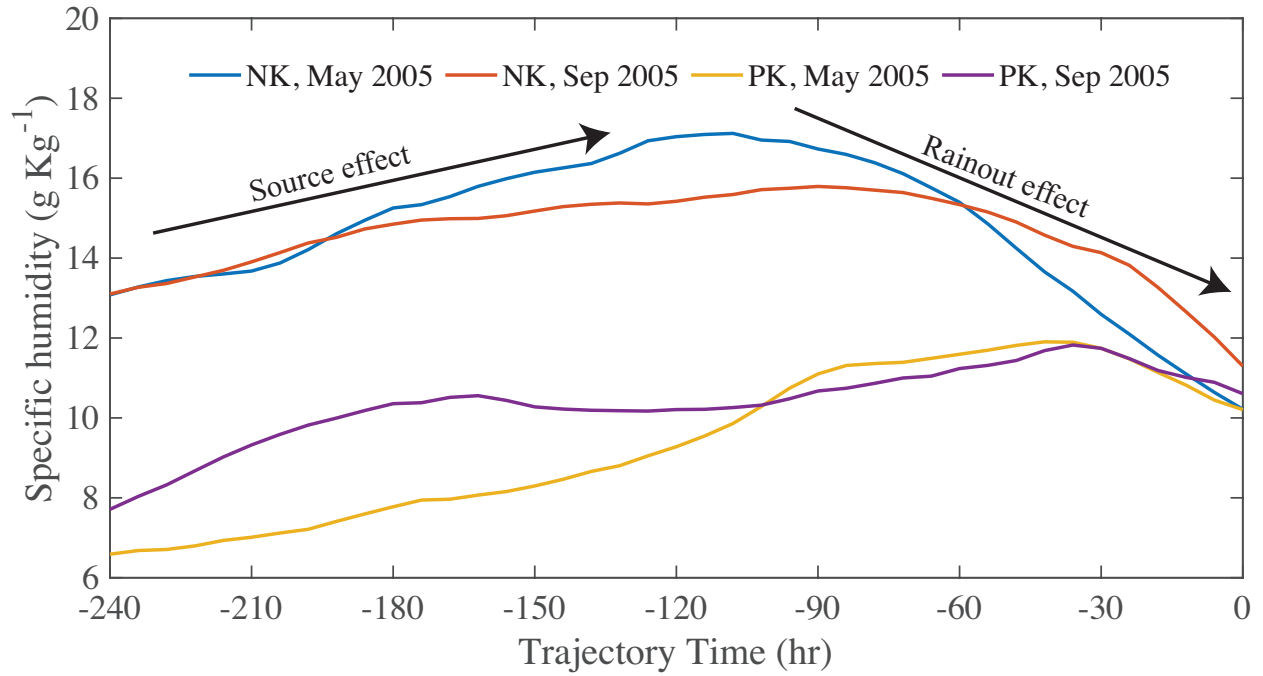


Figure S4. Time evolution of IsoGSM-simulated specific humidity along the air mass back trajectory for NK and PK in May and September.

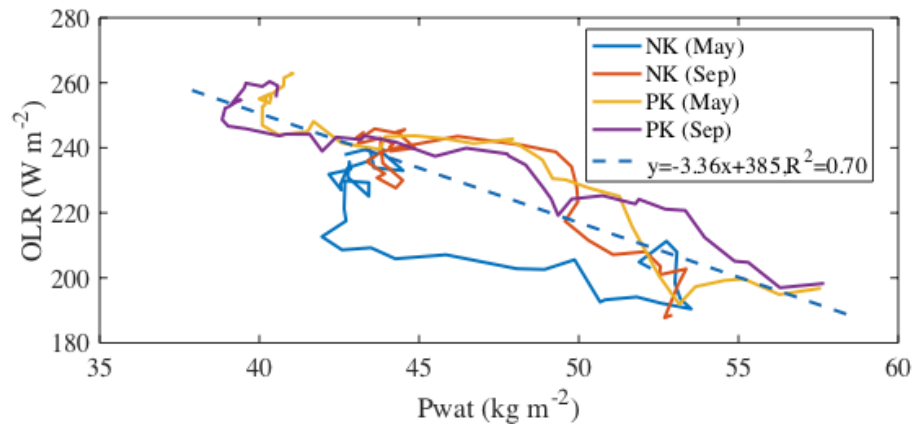


Figure S5. The correlations between OLR and precipitable water content for NK and PK in May and September. The regression (dash line) estimated from four months data mentioned above.

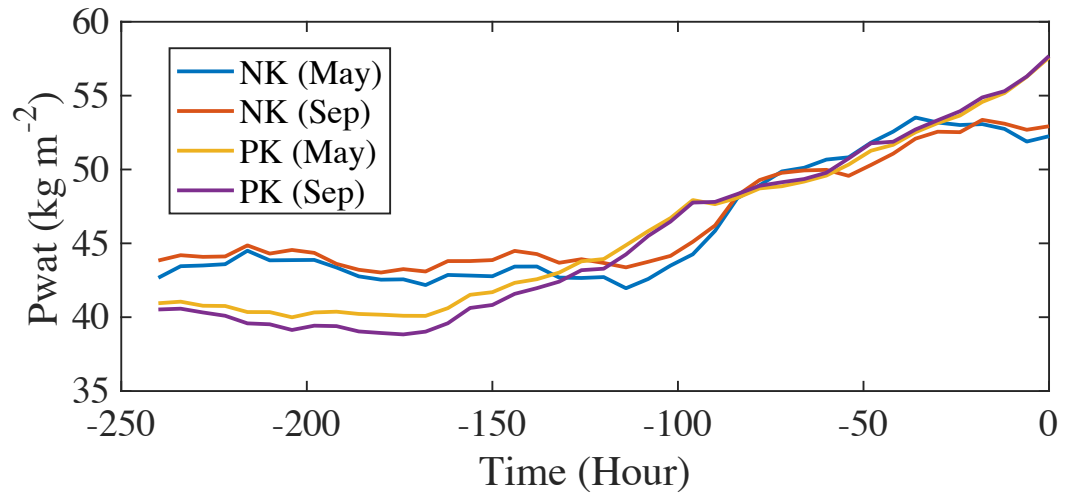


Figure S6. Time evolution of IsoGSM-simulated precipitable water content along the airmass back trajectory for NK and PK in May and September.

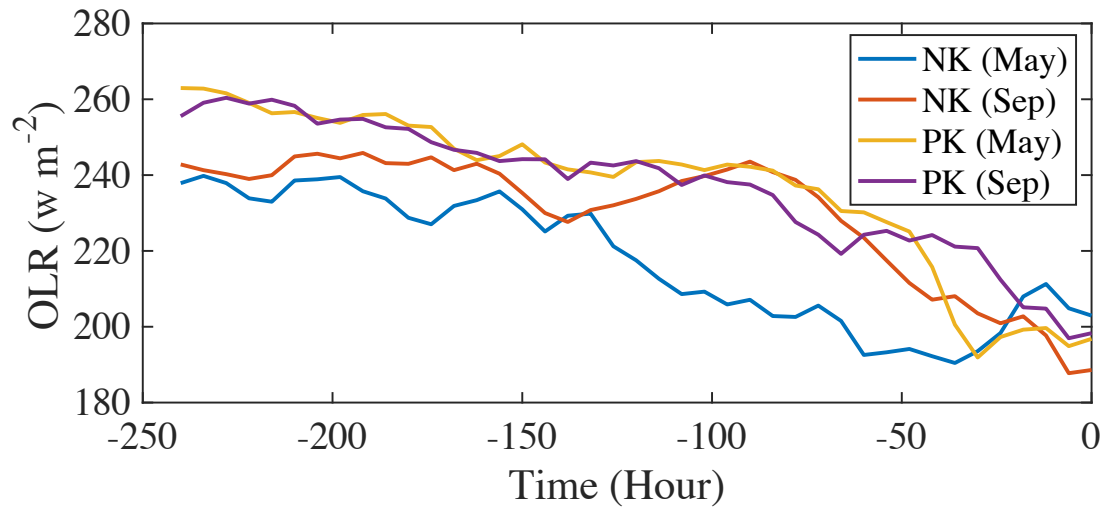


Figure S7. Time evolution of observed outgoing longwave radiation along the air mass back trajectory for NK and PK in May and September.



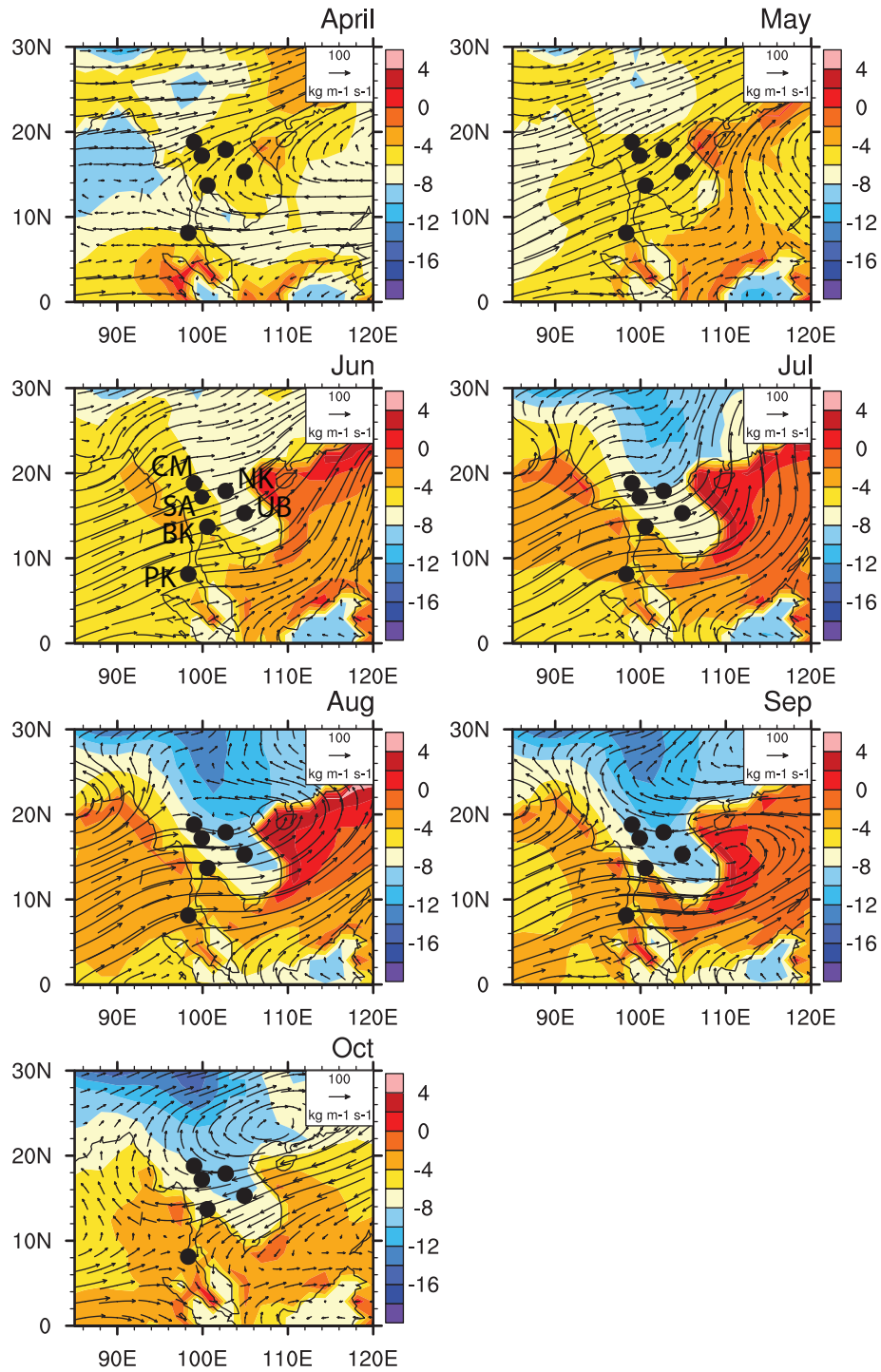


Figure S8. IsoGSM-simulated spatial distribution of seasonal means of vertical integral water vapor (water vapor transport integrated between the surface layer to 300 hPa level) transport (plotted as vectors) and evaporation  $\delta^{18}\text{O}$  isotope ratios (plotted as shading) from 2003 to 2013.

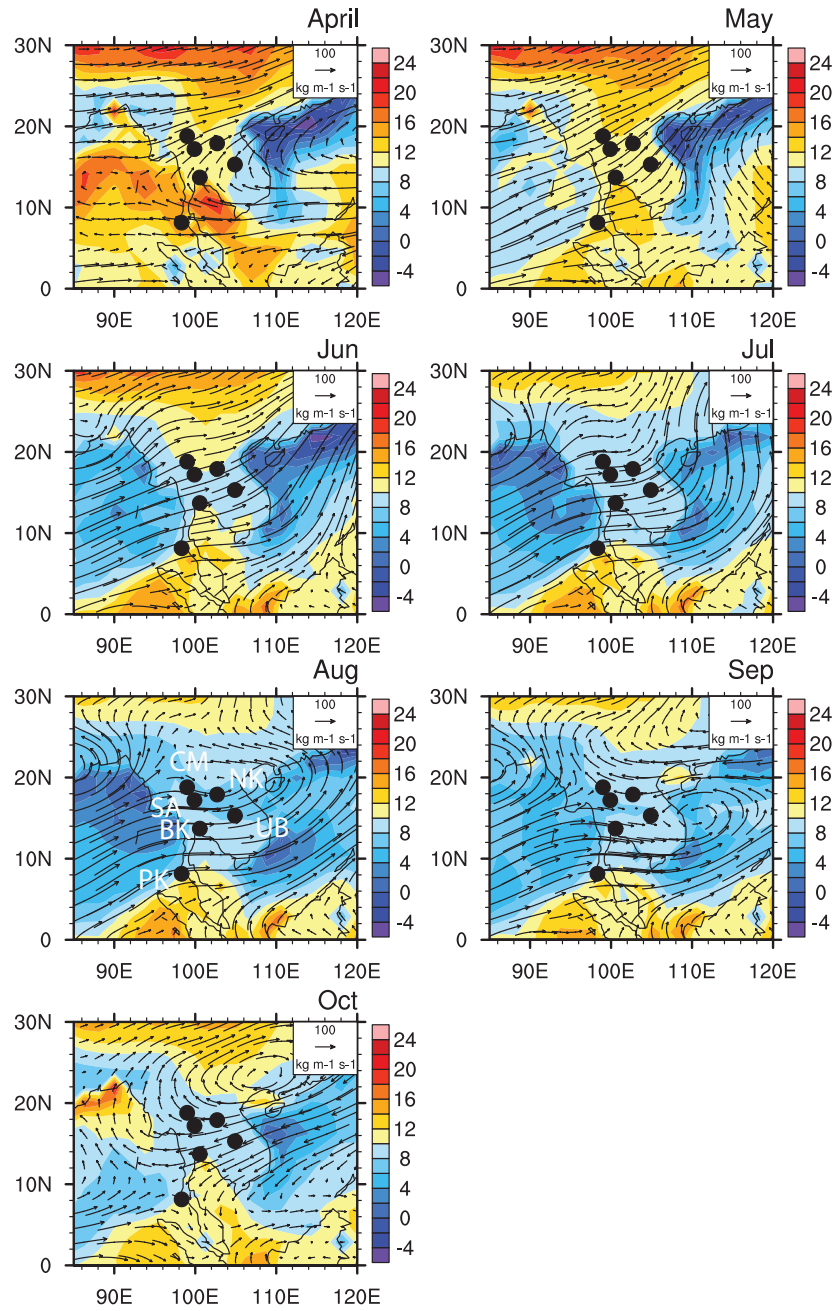


Figure S9. IsoGSM-simulated spatial distribution of seasonal means of vertical integral water vapor (water vapor transport integrated between the surface layer to 300 hPa level) transport (plotted as vectors) and evaporation d-excess isotope ratios (plotted as shading) from 2003 to 2013.

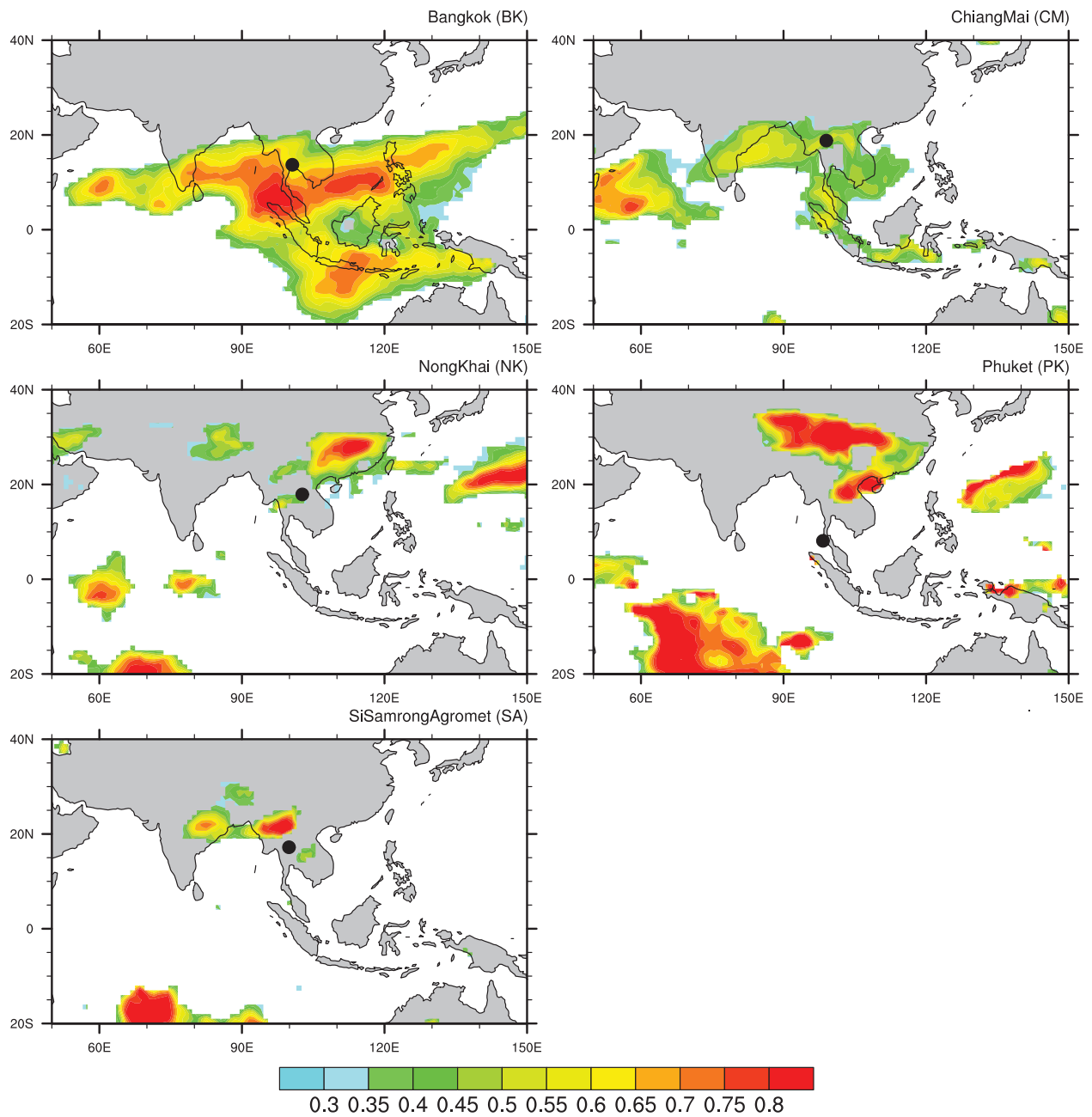


Figure S10. Spatial distribution of correlation coefficients (R) between monthly precipitation  $\delta^{18}\text{O}$  and OLR for DJF season. Only areas with  $R > 0.3$  are shown.